remote sensing

MDPI

Article

An Empirical Atmospheric Weighted Average Temperature Enhancement Model in the Yunnan–Guizhou Plateau Considering Surface Temperature

Yi Shen [1], Peicheng Li [1], Bingbing Zhang [1,*], Tong Wu [1], Junkuan Zhu [1], Qing Li [1] and Wang Li [2]

[1] School of Geographic Sciences, Xinyang Normal University, Xinyang 464000, China; shenyi@xynu.edu.cn (Y.S.); lipeicheng@xynu.edu.cn (P.L.); tongwu@xynu.edu.cn (T.W.); zhujunkuan@xynu.edu.cn (J.Z.); liqing@xynu.edu.cn (Q.L.)

[2] Faculty of Land Resources Engineering, Kunming University of Science and Technology, Kunming 650093, China; liwang@kust.edu.cn

* Correspondence: bbzhang@whu.edu.cn; Tel.: +86-188-2738-0309

Abstract: Atmospheric weighted mean temperature (Tm) is a crucial parameter for retrieving atmospheric precipitation using the Global Navigation Satellite System (GNSS). It plays a significant role in GNSS meteorology research. Although existing empirical models can quickly obtain Tm values for the Yunnan–Guizhou Plateau, their accuracy is generally low due to the region's complex environmental and climatic conditions. To address this issue, this study proposes an enhanced empirical Tm model tailored for the Yunnan–Guizhou Plateau. This new model incorporates surface temperature (Ts) data and employs the least squares method to determine model coefficients, thereby improving the accuracy of the Tm empirical model. The research utilizes observational data from 16 radiosonde stations in the Yunnan–Guizhou Plateau from 2010 to 2018. By integrating Ts into the Hourly Global Pressure and Temperature (HGPT2) model, we establish the enhanced empirical Tm model, referred to as YGTm. We evaluate the accuracy of the YGTm model using Tm values obtained from the 2019 radiosonde station measurements as a reference. A comparative analysis is conducted against the Bevis model, the HGPT2 model, and the regional linear model LTm. The results indicate that at the modeling stations, the proposed enhanced model improves Tm prediction accuracy by 24.9%, 16.1%, and 22.4% compared to the Bevis, HGPT2, and LTm models, respectively. At non-modeling stations, the accuracy improvements are 26.2%, 17.1% and 24.4%, respectively. Furthermore, the theoretical root mean square error and relative error from using the YGTm model for GNSS water vapor retrieval are 0.27 mm and 0.93%, respectively, both of which outperform the comparative models.

Keywords: atmospheric weighted average temperature; least squares method; Yunnan–Guizhou Plateau region; global satellite navigation positioning system

check for updates

Citation: Shen, Y.; Li, P.; Zhang, B.; Wu, T.; Zhu, J.; Li, Q.; Li, W. An Empirical Atmospheric Weighted Average Temperature Enhancement Model in the Yunnan–Guizhou Plateau Considering Surface Temperature. *Remote Sens.* **2024**, *16*, 4366. https://doi.org/10.3390/rs16234366

Academic Editors: Jose Moreno and Yuriy Kuleshov

Received: 14 October 2024
Revised: 5 November 2024
Accepted: 19 November 2024
Published: 22 November 2024

Copyright: © 2024 by the authors. Licensee MDPI, Basel, Switzerland. This article is an open access article distributed under the terms and conditions of the Creative Commons Attribution (CC BY) license (https://creativecommons.org/licenses/by/4.0/).

1. Introduction

Water vapor plays a crucial role in the atmospheric system, influencing both weather and climate changes, as well as the formation and evolution of extreme weather events. Initially, scientists utilized technologies such as radiosondes, microwave radiometers, and medium-resolution imaging spectrometers to measure atmospheric water vapor content [1,2]. While these methods effectively quantified water vapor, they had relatively low temporal and spatial resolution. In recent years, the rapid development of GNSS technology has expanded the applications for detecting water vapor changes [3]. Compared to traditional methods, GNSS atmospheric water vapor detection offers significant advantages, including high temporal and spatial resolution, low cost, all-weather capability, and high accuracy. Consequently, GNSS atmospheric water vapor detection has become a focal point of research for scholars both domestically and internationally [4–6].

When processing GNSS data, it is possible to calculate the Zenith Total Delay (ZTD) in the troposphere [7]. By subtracting the Zenith Hydrostatic Delay (ZHD), obtained from models, from the ZTD, researchers can derive the Zenith Wet Delay (ZWD), which is directly related to Precipitable Water Vapor (PWV). To obtain PWV, the ZWD must be multiplied by a conversion coefficient, denoted as Π [8–10]. Consequently, investigating the accuracy of this conversion coefficient is crucial for utilizing GNSS to detect PWV. The precision of the conversion coefficient is essential for accurately retrieving atmospheric PWV, and its determination is primarily influenced by the atmospheric Tm [11–15]. Therefore, developing an accurate Tm model is particularly important for the retrieval of atmospheric PWV.

Researchers both domestically and internationally have conducted extensive studies on Tm modeling. Reference [16] collected data from 13 U.S. radiosonde stations located between 27°N and 65°N, analyzing 8718 profiles. The study found a strong linear relationship between Tm and Ts, leading to the development of the widely used Bevis model. Although the geographical and seasonal variations in Ts can reflect those in Tm, the Bevis model often exhibits regional accuracy discrepancies in practical applications. Consequently, scholars have developed corresponding linear regression models for Tm and Ts tailored to different regions [17–20].

Several researchers have developed empirical Tm models that account for station location and temporal information, based on local or global multi-year Tm data [21–23]. For instance, based on GPT [24], GPT2 [25], GPT2w [26], and GPT3 [27], GWMT [28], GTm-II [29], and GTm-III [30] models of Tm were determined in combination with ground point coordinates and time. The GPT3 models derived from the reanalysis of numerical prediction products provided by the European Centre for Medium-Range Weather Forecasts (ECMWF) have a maximum spatial resolution of 1° × 1° and a maximum time resolution of 6 h [27]. Under the low resolution of the model, the temperature, pressure, and water vapor may change greatly. The HGPT2 model [31] based on the 20-year fifth-generation ECMWF (ERA5) reanalysis data overcomes these limitations. Linear regression is used to estimate the weighted average temperature from the surface temperature, taking into account the periodic change function and a linear trend to illustrate the global climate change scenario. Its spatial and temporal resolution are 1 h and 0.25° × 0.25°. The HGPT2 model offers advantages such as open-source accessibility, user-friendliness, and high temporal resolution. These features position HGPT2 as a promising alternative to the GPT3 model, potentially delivering high-resolution tropospheric parameters for global regions. Although the HGPT2 model can provide high spatiotemporal resolution data for Ts and Tm, its accuracy is still inferior to that of radiosonde data. While radiosonde data are highly accurate, their sparse distribution limits comprehensive coverage. Therefore, this study aims to develop a regionally enhanced atmospheric weighted average temperature model by integrating the high spatiotemporal resolution of the HGPT2 model with the high accuracy of radiosonde data, thereby improving the model's predictive accuracy.

To address the complex geographical and climatic conditions of the Yunnan–Guizhou Plateau, this study proposes an enhanced empirical Tm model to improve model accuracy and adaptability in the region. The model is based on the HGPT2 framework and incorporates Ts data, using the least squares method to quickly obtain refinement coefficients for error compensation in the Tm values of the HGPT2 model. This enhancement significantly improves the Tm model accuracy of the HGPT2 model, which is crucial for enhancing the precision of GNSS water vapor retrieval in the Yunnan–Guizhou Plateau.

2. Research Area and Data Sources

2.1. Research Area

The Yunnan–Guizhou Plateau is located in the southwestern region of China, approximately between 100°–111° East longitude and 22°–30° North latitude. The topography of the area is complex, with altitudes generally ranging from 400 to 3500 m. The region has a plateau monsoon climate with distinct dry and wet seasons and minimal temperature change throughout the year. Annual precipitation typically ranges from 600 to 2000 mm,

with an uneven spatial distribution. Notably, 85% to 95% of the annual precipitation occurs between April and October, often leading to flooding disasters. Conversely, the dry season is prolonged, increasing the risk of seasonal droughts.

The average annual temperature varies between 5 °C and 24 °C, exhibiting a trend of higher temperatures in the south and lower temperatures in the north. The differences in natural conditions contribute to a rich diversity of vegetation and soil types across the plateau, with a clear zonal distribution. Therefore, studying the enhanced model of experience-weighted average temperature in the Yunnan–Guizhou Plateau is of significant importance for precipitation warning and meteorological forecasting.

2.2. Data Sources

The observation data from radiosonde stations was provided by the University of Wyoming, http://www.weather.uwyo.edu/upperair/sounding.html (accessed on 20 September 2024). These data include atmospheric profiling conducted twice daily at 00:00 and 12:00, encompassing relevant meteorological information such as pressure, temperature, dew point temperature, and relative humidity, along with the locations of the measurement stations. Using numerical integration methods, Tm values can be calculated from different isobaric surfaces, while Ts values can be derived from the radiosonde data. This study selected observational data from 16 radiosonde stations evenly distributed across the Yunnan–Guizhou Plateau from 2010 to 2018 to enhance the model. Accuracy assessments were conducted using measured data from 16 modeling and 7 non-modeling radiosonde stations in 2019. The specific locations of the radiosnde stations are illustrated in Figure 1.

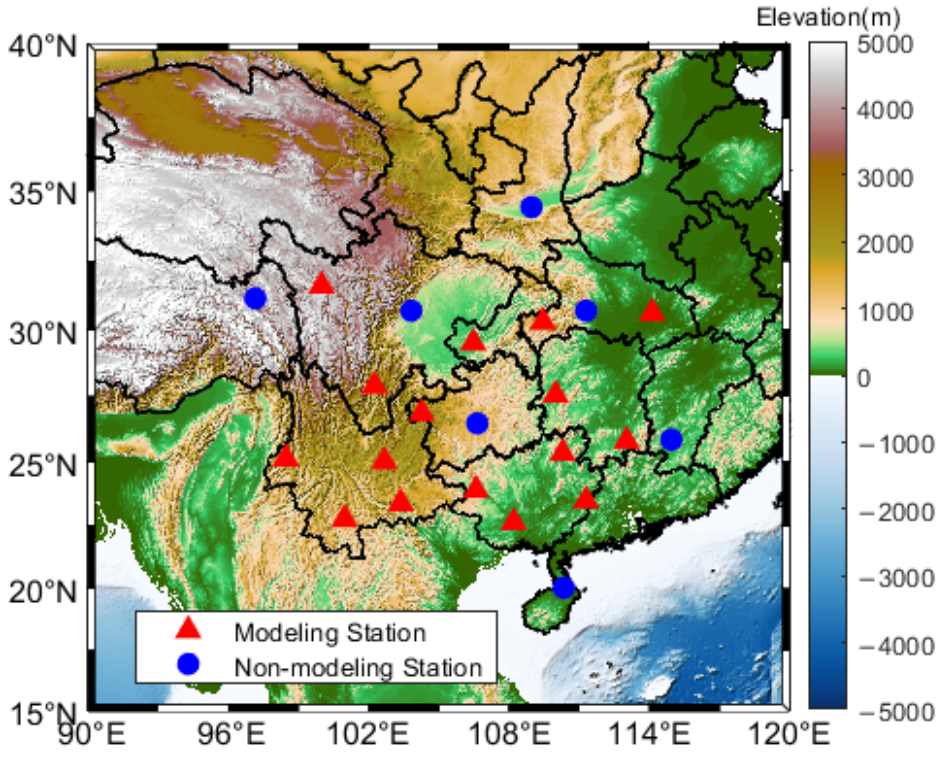


Figure 1. The distribution of radiosonde stations in the Yunnan-Guizhou Plateau region, with red circles representing modeling stations and blue triangles indicating non-modeling stations.

The Tm at the radiosonde station can be calculated through numerical integration using the water vapor pressure (e) and absolute temperature (T), as detailed in Equation (1).

Reference [23] provides a comprehensive explanation of the definition and calculation methods for Tm.

$$T_m = \frac{\int \frac{e}{T} dZ}{\int \frac{e}{T^2} dZ} \tag{1}$$

In Equation (1), e represents the vapor pressure in hPa, and T denotes the absolute temperature in K. After discretizing Equation (1), it can be used for the precise calculation of Tm, as detailed in Equation (2).

$$T_m = \frac{\sum_{i=1}^{N} \frac{e_i}{T_i} \Delta h_i}{\sum_{i=1}^{N} \frac{e_i}{T_i^2} \Delta h_i} \tag{2}$$

In Equation (2), i denotes the i-th layer. The variables e_i and T_i represent the water vapor pressure and atmospheric temperature of the i-th layer, respectively, while indicating the height difference between adjacent pressure layers.

2.3. Existing Tm Models

(1) Bevis model

Bevis et al. [16] analyzed the data from 13 radiosonde stations in the United States and found a strong linear correlation between Tm and the station temperature Ts. They proposed representing Tm as a linear function of Ts, which simplifies the process of obtaining Tm. To achieve more accurate Tm values, Bevis et al., developed the Bevis regression model based on an analysis of 8717 radiosonde data points, as shown in Equation (3).

$$T_m = 70.2 + 0.72 \cdot T_s \tag{3}$$

In Equation (3), both T_m and T_s are measured in Kelvin (K). The Bevis model has been widely applied in ground-based GNSS water vapor detection.

(2) HGPT2 model

Mateus et al. [31] developed the HGPT2 model utilizing 20 years of data from the ERA5 reanalysis. This model generates key variables such as Ts, surface pressure, ZHD, and Tm. The HGPT2 model employs a time-segmentation approach, extracting simulations every hour from the 1 h temporal resolution time series. This process results in 24 distinct time series, one for each hour of the day, thereby achieving a 24 h temporal resolution for each grid point. Using Fourier analysis, the model calculates various global coefficients for surface air temperature and pressure at each hour and grid point, taking into account both location and time. Additionally, a linear trend is incorporated to reflect local long-term temperature changes. For Ts, the model considers three periodic functions to capture annual, semi-annual, and quarterly variations, as outlined in Equation (4). The HGPT2 model integrates these equations to accurately represent Ts dynamics.

$$\begin{aligned} T_s = {} & a^h + b^h \cdot (t - t_0) + a_1^h \cdot \cos\left(\tfrac{2\pi(t-t_0)}{365.25} + f_1^h\right) \\ & + a_2^h \cdot \cos\left(\tfrac{2\pi(t-t_0)}{182.63} + f_2^h\right) + a_3^h \cdot \cos\left(\tfrac{2\pi(t-t_0)}{91.31} + f_3^h\right) \end{aligned} \tag{4}$$

In Equation (4), t and t_0 represent the modified Julian date (MJD) and the date of the first observation, respectively. The variable h indicates the time in Coordinated Universal Time (UTC) derived from t. The coefficients a_1, a_2, and a_3 correspond to the annual, semi-annual, and quarterly amplitudes, respectively. Similarly, the coefficients f_1, f_2, and f_3 represent the annual, semi-annual, and quarterly phases. Additionally, a and b are the regression coefficients. For each hour and the specified geographic location, the amplitudes, initial phases, and linear coefficients are bilinearly interpolated. The Tm can be expressed

as a linear function of the T_s. Accurate estimation of the Tm is crucial for ensuring reliable precipitable water vapor (PWV) measurements. To calculate the value of Tm, we utilize Equation (5).

$$T_m = \alpha + \beta \cdot T_s \tag{5}$$

In Equation (5), α and β represent the linear regression coefficients. To address the seasonality and geographic variability inherent in Tm, these coefficients are estimated using a time series of surface air temperature and air temperature (in K) from ERA5.

(3) LTm model

This study constructs a linear weighted average temperature model (LTm) for the Yunnan–Guizhou Plateau using Ts and Tm data from 16 monitoring stations between 2010 and 2018, as detailed in Equation (6).

$$T_m = 75.4 + 0.70 \cdot T_s \tag{6}$$

3. Construction of an Enhanced Tm Model for the Yunnan–Guizhou Plateau Region

This study analyzes radiosonde data from 16 modeling stations in the Yunnan–Guizhou Plateau region between 2010 and 2018. By examining the differences between the measured Tm and the estimated Tm by the HGPT2 model, as well as the discrepancies between the measured Ts and the estimated Ts by the HGPT2 model, a correlation analysis was conducted. The results indicate a linear correlation coefficient of 0.63, as shown in Figure 2. Consequently, this paper proposes an empirical enhancement model, YGTm, which incorporates the measured Ts, with the specific model formulation presented in Equation (7).

$$YGT_m = T_m^{HGPT2} + a \cdot (T_s - T_s^{HGPT2}) + b \tag{7}$$

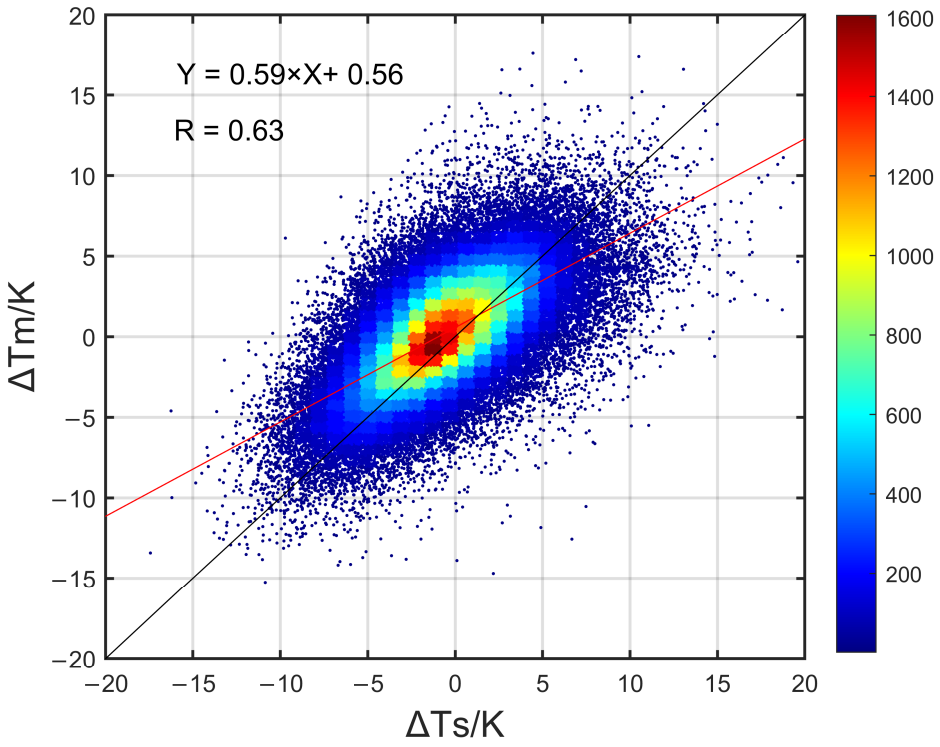


Figure 2. Scatter plot of Tm and Ts differences.

In Equation (7), a and b are model coefficients, T_m^{HGPT2} represents the Tm value estimated by the HGPT2 model, T_s^{HGPT2} denotes the Ts value estimated by the HGPT2 model, and Ts is the measured Ts. This study utilizes radiosonde data from 16 modeling

stations in the Yunnan–Guizhou Plateau region from 2010 to 2018, applying the HGPT2 model and solving it using the least squares method [32,33]. The specific model for YGTm is presented in Equation (8).

$$YGT_m = T_m^{HGPT2} + 0.5855 \cdot (T_s - T_s^{HGPT2}) + 0.5582 \quad (8)$$

4. Evaluation of the Accuracy of the Tm Model

This study primarily uses two metrics, bias and root mean square error (RMS), to evaluate the weighted average temperature model for the Yunnan–Guizhou Plateau. The specific calculation formulas are presented in Equations (9) and (10).

$$\text{bias} = \frac{1}{M}\sum_{m=1}^{M}(\text{Tm}_{model}^{m} - \text{Tm}_{radiosonde}^{m}) \quad (9)$$

$$RMS = \sqrt{\frac{1}{M}\sum_{m=1}^{M}(\text{Tm}_{model}^{m} - \text{Tm}_{radiosonde}^{m})^2} \quad (10)$$

In Equations (9) and (10), M represents the total number of samples, Tm_{model}^{m} denotes the Tm values derived from the empirical models (the Bevis model, LTm model, HGPT2 model, and YGTm model), and $\text{Tm}_{radiosonde}^{m}$ indicates the high-precision Tm values obtained from radiosonde observations using the numerical integration method.

4.1. Accuracy Analysis of the Tm Model for Modeling Stations in 2019

Using the 2019 radiosonde data from 16 modeling stations in the Yunnan–Guizhou Plateau, we obtained Tm as a reference value through integration methods to validate the accuracy of the enhanced Tm model, YGTm. Additionally, we compared the results of the YGTm model with those from the widely used Bevis model, the regional linear model LTm, and the HGPT2 model. We calculated and analyzed the bias and RMS values, with detailed results presented in Table 1, and Figures 3 and 4.

Table 1. Assessment of error statistics for various Tm models using the 2019 modeling station radiosonde data.

Model	Bias/K			RMS/K		
	Minimum Value	Maximum Value	Mean Value	Minimum Value	Maximum Value	Mean Value
Bevis	−4.01	5.21	−0.72	2.28	6.17	3.41
HGPT2	−1.62	0.74	−0.44	2.27	4.08	3.05
LTm	−3.42	5.97	−0.14	2.28	6.82	3.30
YGTm	−1.99	2.09	−0.13	1.84	4.00	2.56

The statistical results in Table 1 show that the average bias values of the LTm and YGTm models considering local radiosonde data are −0.14 and −0.13 K, respectively, which is significantly less than that of the Bevis and HGPT2 models. The average RMS values of the Bevis, HGPT2, LTm, and YGTm models are 3.41, 3.05, 3.30 and 2.56 K, respectively. The maximum RMS of HGPT2 and YGTm for modeling stations are 4.08 and 4.00 K, respectively. Considering the average bias and average RMS, the linear models such as the Bevis model and the regional linear model LTm fluctuate greatly and cannot reflect the nonlinear variation characteristics of Tm. The HGPT2 model, developed from ERA5 data, significantly enhances Tm model accuracy relative to the LTm and Bevis models. The proposed YGTm model takes into account the regional characteristics and high-precision radiosonde data, and it performs best among the four models. The accuracy of the YGTm model surpasses that of the Bevis, HGPT2, and LTm models at 24.9%, 16.1%,

and 22.4%, respectively. This demonstrates that the YGTm model has better adaptability to Tm estimation in the Yunnan–Guizhou Plateau region.

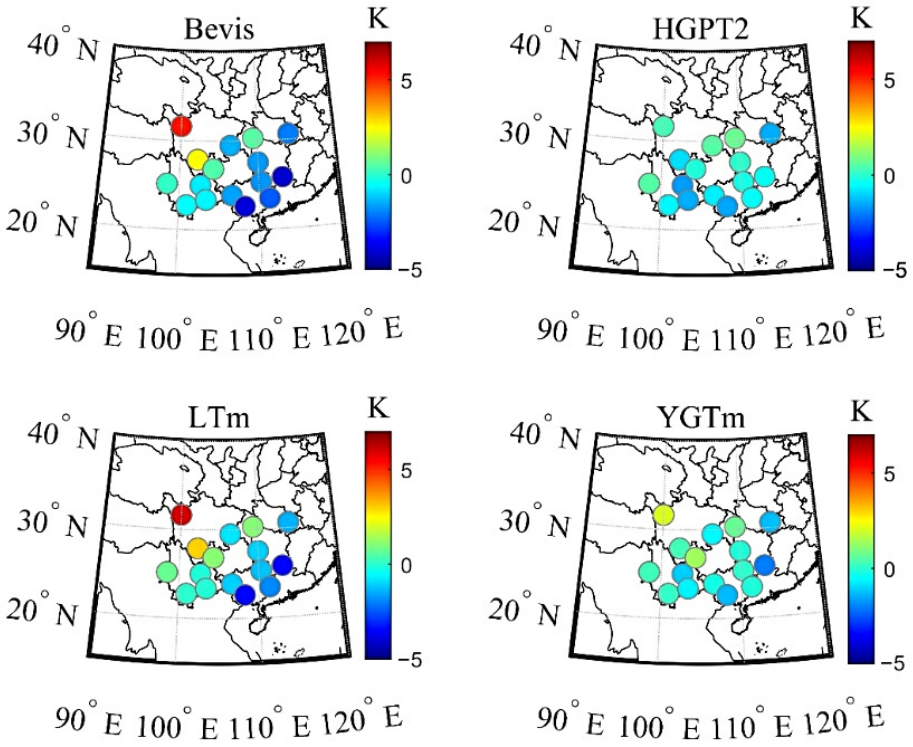


Figure 3. Evaluation of the bias distribution maps for various Tm models using modeling station data from 2019.

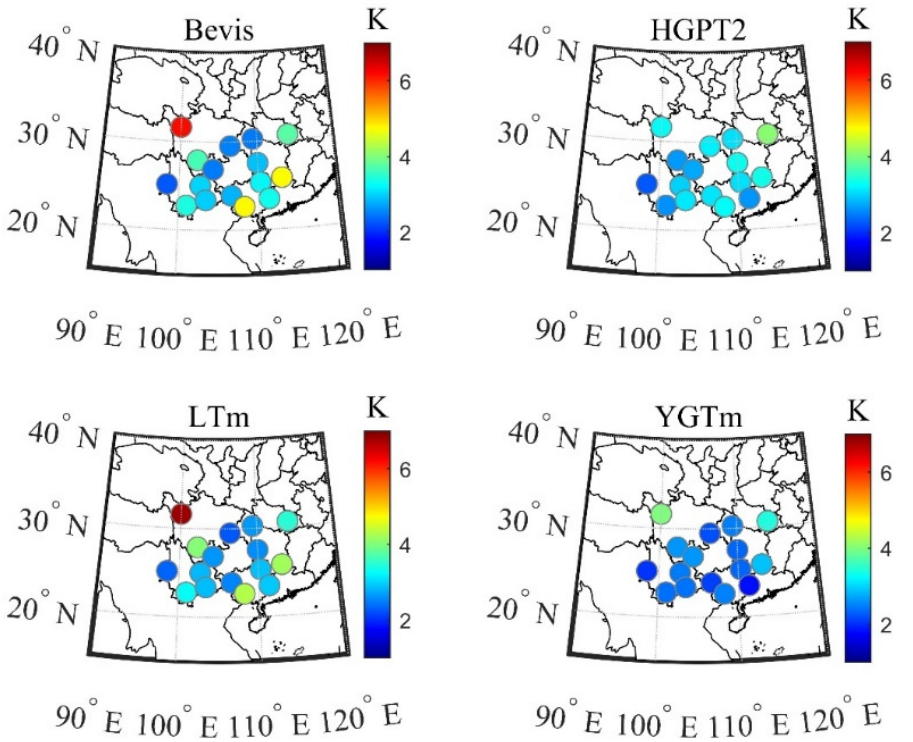


Figure 4. Evaluation of the RMS distribution maps for various Tm models using modeling station data from 2019.

Figure 3 shows that the Bevis model exhibits significant negative bias at most measurement stations in the Yunnan–Guizhou Plateau, with a few stations displaying notable positive bias. The HGPT2 model shows both positive and negative biases, but negative biases are more prevalent than positive ones. The LTm model demonstrates clear positive and negative biases, although its overall average bias is relatively small. In contrast, the YGTm model has minimal and more uniform biases in the Yunnan–Guizhou Plateau, indicating that it has smaller and more stable biases compared to the other three models.

According to the analysis in Figure 4, both the Bevis and LTm models exhibit relatively high RMS values in the Yunnan–Guizhou Plateau region. In contrast, the HGPT2 model demonstrates improved model accuracy compared to the Bevis and LTm models. The YGTm model, however, shows smaller and more stable overall RMS values, outperforming the other three models. These results indicate that the YGTm model possesses superior stability and model accuracy in the Yunnan–Guizhou Plateau region.

To evaluate the seasonal performance of four selected models, this study analyzed the daily bias and RMS values of these Tm models. The results, illustrated in Figure 5, reveal significant findings. The Bevis and HGPT2 models exhibited substantial negative bias on most days throughout 2019 over the Yunnan–Guizhou Plateau region, with pronounced values during spring and winter. This indicates a significant systematic bias in the calculation of Tm for these models. Conversely, the LTm model demonstrated a relatively clear positive bias in the spring and a notable negative bias in the summer. The YGTm model, however, displayed smaller bias values with no evident seasonal variation throughout the year. Regarding RMS values, all models showed distinct seasonal variations, with larger RMS values during spring and winter and smaller values during summer. This pattern can be attributed to the location of the most selected radiosonde stations in middle latitudes, where Tm exhibits less variation in summer and more in winter [22,34]. Notably, the YGTm model consistently had smaller RMS values compared to the other models for most days in 2019 over the Yunnan–Guizhou Plateau region. In summary, the YGTm model demonstrated more stable and smaller RMS values than the other selected Tm models.

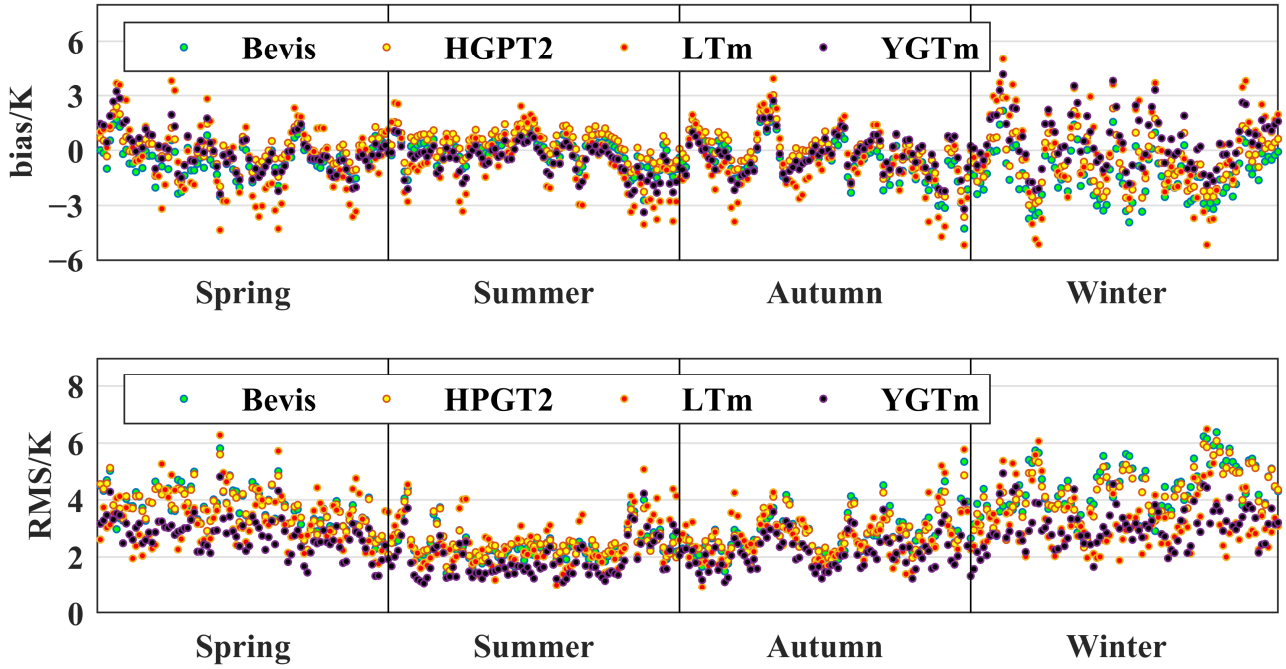


Figure 5. Results of the daily bias and RMS values for four Tm models using modeling station data from 2019.

4.2. Accuracy Analysis of the Tm Model for Non-Modeling Stations in 2019

To further validate the generalization capability of the YGTm model in the Yunnan–Guizhou Plateau region, this study selected seven radiosonde stations as non-modeling sites. We utilized the radiosonde data from these non-modeling stations in 2019 to calculate Tm as a reference value using the integration method, thereby assessing the forecast accuracy of the enhanced Tm model, YGTm. Additionally, we compared the forecast results of the YGTm model with those from the widely used Bevis model, the regional linear model LTm, and the HGPT2 model. We calculated and reported the bias and RMS values, with detailed results presented in Table 2, and Figures 6 and 7.

Table 2. Evaluation of error statistics for various Tm models using non-modeling station radiosonde data from 2019.

Model	Bias/K			RMS/K		
	Minimum Value	Maximum Value	Mean Value	Minimum Value	Maximum Value	Mean Value
Bevis	−3.66	5.53	−0.49	2.75	6.50	3.82
HGPT2	−1.78	1.48	−0.60	3.09	4.00	3.40
LTm	−3.20	6.26	0.11	2.77	7.13	3.73
YGTm	−1.13	1.58	−0.37	2.16	3.65	2.82

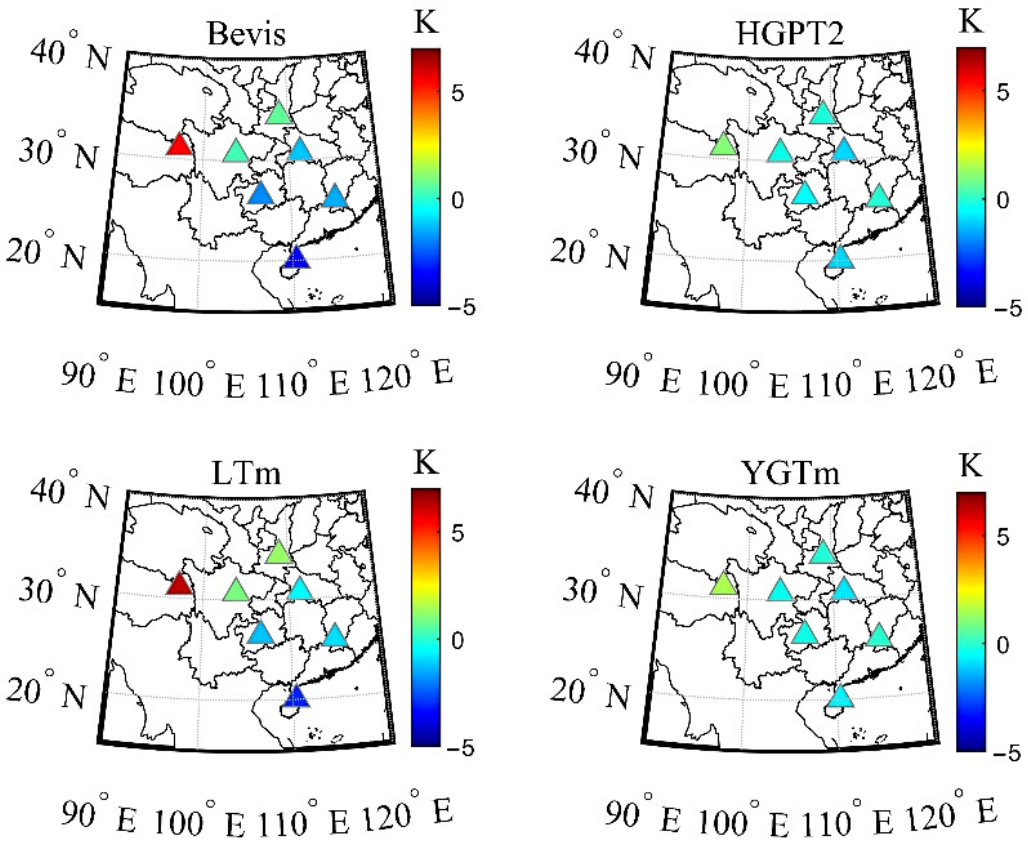


Figure 6. The bias distribution maps for various Tm models using non-modeling station data from 2019.

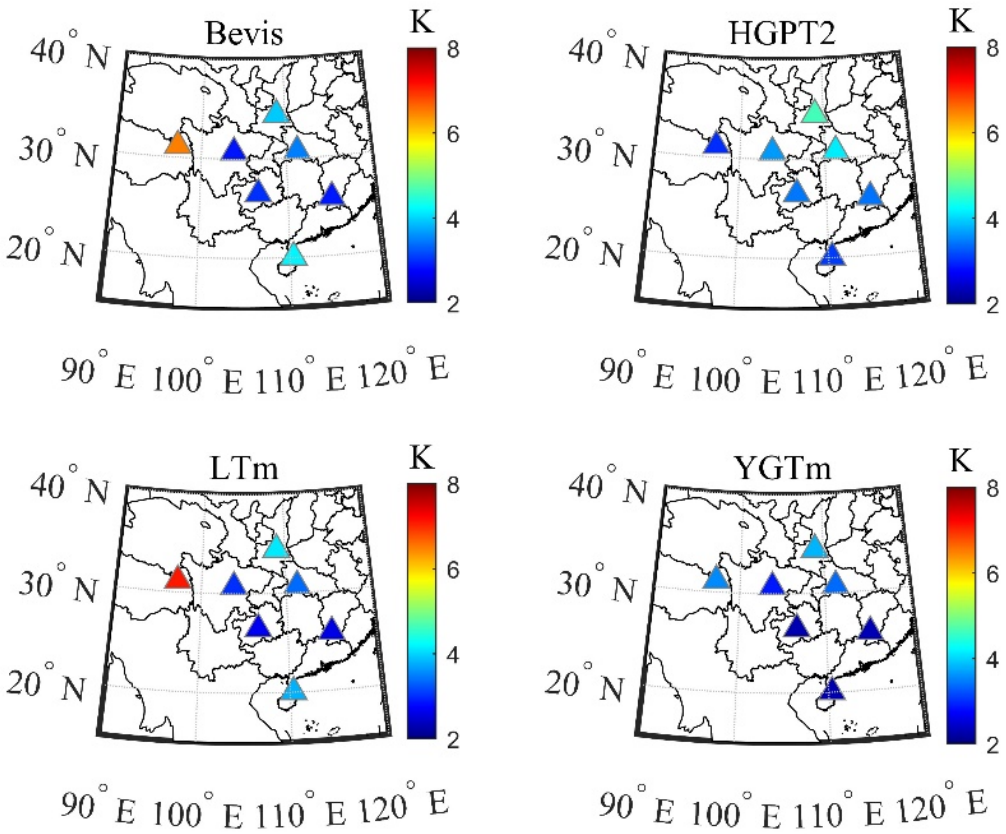


Figure 7. The RMS distribution maps for various Tm models using non-modeling station data from 2019.

According to the data presented in Table 2, the Bevis, HGPT2, and LTm models exhibit significant negative biases at non-modeling sites, with average bias values of −0.49 K, −0.60 K, and 0.11 K, respectively. This indicates a clear systematic bias in the calculation of Tm by these three models in the Yunnan–Guizhou Plateau region. In contrast, the YGTm model shows a maximum bias of 1.58 K and a minimum bias of −1.13 K, resulting in an average bias of −0.37 K, which is the smaller absolute bias among the four models. Regarding RMS, the Bevis model has the highest average RMS value of 3.82 K, while the YGTm model has the lowest average RMS value of only 2.82 K. The regional linear model LTm demonstrates improved accuracy compared to the Bevis model, suggesting that the LTm model, built on localized radiosonde data, offers greater reliability. Furthermore, the HGPT2 model shows improvements in both bias and RMS values compared to the Bevis and LTm models, without exhibiting excessive bias or RMS values. This indicates that the HGPT2 model, developed using high-resolution and high-quality ERA5 data, significantly enhances Tm model accuracy relative to the LTm and Bevis models. Notably, the model accuracy of the YGTm model surpasses that of the Bevis, HGPT2, and LTm models by 26.2%, 17.1%, and 24.4%, respectively. This demonstrates that the YGTm model performs markedly better in estimated Tm in the Yunnan–Guizhou Plateau region, particularly enhancing the predictive capability compared to the HGPT2 model.

According to the results in Figure 6, the Bevis model exhibits a significant negative bias at most monitoring stations in the Yunnan–Guizhou Plateau, while a few stations show notable positive bias. The HGPT2 model displays alternating positive and negative biases, with a greater number of stations exhibiting negative bias than positive. The LTm model shows pronounced positive and negative biases, but its overall average bias is relatively small. In contrast, the YGTm model demonstrates both smaller and more uniformly distributed biases in the Yunnan–Guizhou Plateau, indicating that it has lower and more stable biases compared to the other three models.

Analysis of Figure 7 indicates that both the Bevis and LTm models exhibit relatively high RMS values in the Yunnan–Guizhou Plateau region. In contrast, the HGPT2 model demonstrates improved model accuracy compared to the Bevis and LTm models. Additionally, the YGTm model shows a smaller and more stable overall RMS when compared to the other three models. These findings suggest that the YGTm model offers better stability and higher model accuracy in the Yunnan–Guizhou Plateau region.

4.3. The Impact of Tm on the Calculated Values of PWV

The model developed for the Yunnan–Guizhou Plateau aims to enhance the accuracy of Tm predictions, ultimately improving the precision of GNSS-derived PWV. However, GNSS reference stations and radiosonde stations are typically not co-located, and most GNSS stations are primarily used for geodetic research without meteorological sensors. This makes it challenging to comprehensively and reliably assess the impact of Tm on GNSS PWV calculations. To address this issue, this study adopts the method for calculating Tm's influence on GNSS PWV proposed in references [14,23] (Equation (11)) and analyzes the results.

$$\frac{RMS_{PWV}}{PWV} = \frac{RMS_{\Pi}}{\Pi} = \frac{k_3 \cdot RMS_{T_m}}{(k_2' + \frac{k_3}{T_m})T_m^2} = \frac{k_3}{(k_2' + \frac{k_3}{T_m})T_m} \cdot \frac{RMS_{T_m}}{T_m} \tag{11}$$

In Equation (11), RMS_{PWV} is defined as the RMS value of PWV, while RMS_{Π} represents the RMS value of the conversion coefficient. Additionally, RMS_{T_m} denotes the RMS value of Tm, and RMS_{PWV}/PWV indicates the relative error of PWV. The results for RMS_{PWV} and RMS_{PWV}/PWV for each model in the Yunnan–Guizhou Plateau region are presented in Table 3, and Figures 8 and 9.

Table 3. Statistical results of RMS_{PWV} and RMS_{PWV}/PWV in 2019 using 23 radiosonde stations over Yunnan–Guizhou Plateau.

Model	RMS_{PWV} (mm)			RMS_{PWV}/PWV (%)		
	Minimum Value	Maximum Value	Mean Value	Minimum Value	Maximum Value	Mean Value
Bevis	0.16	0.68	0.36	0.81	2.40	1.25
HGPT2	0.12	0.47	0.33	0.81	1.43	1.11
LTm	0.17	0.62	0.34	0.80	2.63	1.21
YGTm	0.15	0.39	0.27	0.63	1.48	0.93

Table 3 presents the calculated RMS_{PWV} and RMS_{PWV}/PWV values derived from the 2019 observational data at the radiosonde stations. Figures 8 and 9 illustrate the scatter distribution of these values for four different models across various measurement stations. Notably, the Bevis model and the regional linear model LTm yield higher RMS_{PWV}/PWV values in the Yunnan–Guizhou Plateau region, recorded at 1.25% and 1.21%, respectively. Their corresponding RMS_{PWV} values are 0.36 mm and 0.34 mm. In contrast, the HGPT2 model shows average RMS_{PWV} and RMS_{PWV}/PWV values of 0.33 mm and 1.11%. The YGTm model exhibits the lowest average values, with RMS_{PWV} at 0.27 mm and RMS_{PWV}/PWV at 0.93%. The variability of the YGTm model ranges from 0.63% to 1.48%, indicating a smaller range and lower values compared to other models. Consequently, the YGTm model provides a more accurate Tm value, effectively facilitating the retrieval of PWV over the Yunnan–Guizhou Plateau.

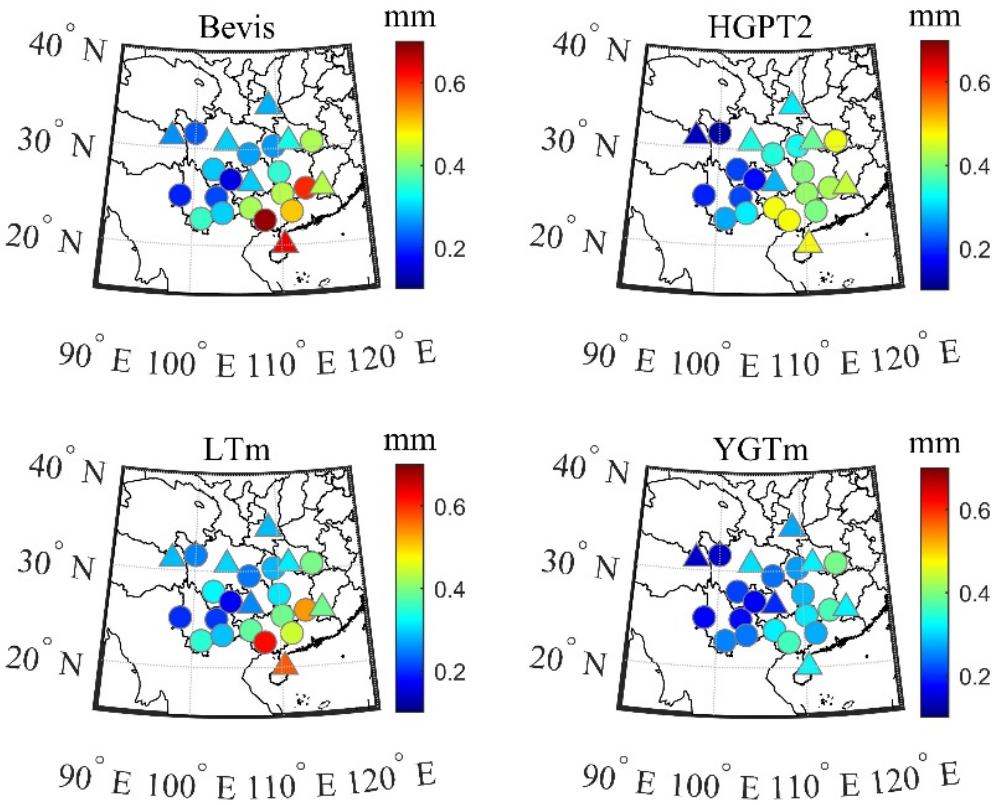


Figure 8. The theoretical RMS of PWV distribution maps for four Tm models using radiosonde data from 2019.

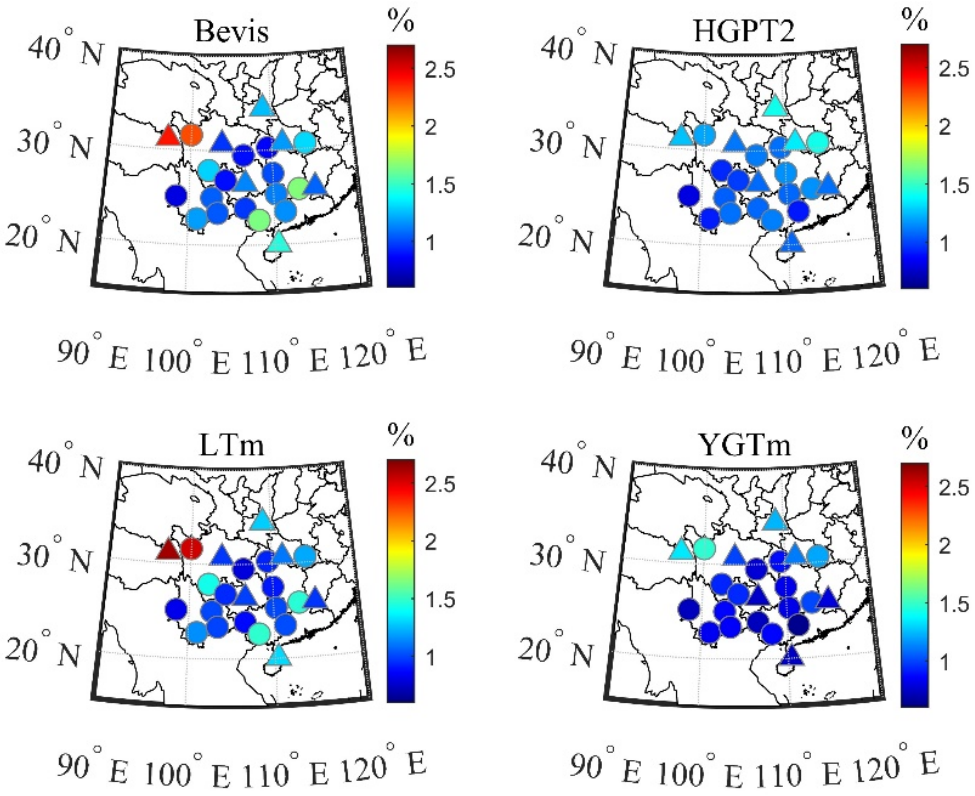


Figure 9. The theoretical relative error of PWV distribution maps for four Tm models using radiosonde data from 2019.

5. Discussion

In this study, the YGTm model was developed by comprehensively considering the HGPT2 model and Ts over the Yunnan–Guizhou Plateau. The YGTm model demonstrated a robust capability to capture the spatiotemporal variations between Tm and its associated factors. The validation of the YGTm proposed in this study and other Tm models, as presented in Section 4, indicates that the ETm model can achieve high accuracy in predictions over the Yunnan–Guizhou Plateau. Several factors contribute to the improvements in the YGTm model over other selected Tm models, as detailed below.

The Bevis model was constructed using two years of observational data from 13 radiosonde stations in the United States to establish a linear relationship between Tm and Ts. However, due to the regional characteristics of the Tm model, the Bevis model exhibits poor adaptability in the Yunnan–Guizhou Plateau region. In contrast, the localized LTm model demonstrates higher accuracy in this area compared to the Bevis model. The HGPT2 model, with a temporal resolution of 1 h and a spatial resolution of $0.25^\circ \times 0.25^\circ$, surpasses the LTm model in both temporal and spatial resolution. Additionally, the HGPT2 model accounts for annual, semi-annual, and seasonal variations, thereby achieving superior model accuracy over the LTm model. The YGTm model integrates the high temporal and spatial resolution of the HGPT2 model with the high-precision ground temperature data from radiosonde stations. By employing the least squares method to estimate model coefficients, the Tm-enhanced YGTm model was developed. This model outperforms both the HGPT2 and LTm models, indicating that enhancing the HGPT2 model with radiosonde data is a valid approach. This not only significantly improves the model accuracy of Tm in the Yunnan–Guizhou Plateau but also provides a valuable methodology for enhancing empirical Tm models in other regions.

6. Conclusions

This study utilizes data from 16 radiosonde stations in the Yunnan–Guizhou Plateau region, collected between 2010 and 2018. Based on the HGPT2 model, a weighted average temperature enhancement model, YGTm, was developed using the least squares method. The accuracy of this model was evaluated in 2019 at both the 16 modeling stations and 7 non-modeling stations. The findings indicate several key results:

(1) A significant correlation exists between the differences in Tm and Ts, with a correlation coefficient of 0.77. At the modeling stations, the YGTm model exhibited an annual mean bias of -0.13 K and an RMS of 2.56 K. This RMS value represents reductions of 24.9%, 16.1%, and 22.4% compared to the Bevis, HGPT2, and regional linear models, respectively.

(2) At the non-modeling stations, the annual mean bias and RMS values were -0.37 K and 2.82 K, respectively. The accuracy (in terms of RMS) improved by 26.2%, 17.1%, and 24.4% when compared to the Bevis, HGPT2, and regional linear models.

(3) An analysis of the impact of different models on the accuracy of GNSS PWV inversion revealed that the YGTm model achieved average RMS_{PWV} and RMS_{PWV}/PWV values of 0.27 mm and 0.93%, respectively. These results surpassed those of the other three models, indicating that the YGTm model demonstrates superior Tm precision.

In summary, the Tm accuracy obtained from the YGTm model is reliable and meets the precision requirements for GNSS atmospheric inversion in the Yunnan–Guizhou Plateau region. This model provides more effective support for meteorological research in the area.

Author Contributions: Conceptualization, Y.S. and B.Z.; methodology, Y.S. and B.Z.; validation, W.L., P.L. and T.W.; data curation, J.Z. and Q.L.; writing—original draft preparation, Y.S.; writing—review and editing, B.Z.; visualization, P.L. and T.W.; supervision, B.Z. and W.L. All authors have read and agreed to the published version of the manuscript.

Funding: This research was funded by the Nanhu Scholars Program for Yong Scholars of XYNU; Key Scientific and Technological Research Project of Henan Province (Grants 232102320280 and 242102320032); the National Natural Science Foundation of China (Grant 42204030); the Yunnan

Fundamental Research Projects (Grants 202201BE070001-035 and 202301AU070062), the Support Programme for Developing Yunnan Talents.

Data Availability Statement: The datasets used and analyzed during the current study are available from the corresponding author on reasonable request. The measured radiosonde observations are obtained from University of Wyoming at http://weather.uwyo.edu/upperair/seasia.html (accessed on 20 September 2024).

Acknowledgments: Thanks to University of Wyoming for the observation data from radiosonde stations.

Conflicts of Interest: The authors declare no conflicts of interest.

References

1. Zhao, Q.; Liu, Y.; Ma, X.; Yao, W.; Yao, Y.; Li, X. An improved rainfall forecasting model based on GNSS observations. *IEEE Trans. Geosci. Remote Sens.* **2020**, *58*, 4891–4900. [CrossRef]
2. Allan, R.P.; Willett, K.M.; John, V.O.; Trent, T. Global changes in water vapor 1979–2020. *J. Geophys. Res. Atmos.* **2022**, *127*, e2022JD036728. [CrossRef]
3. Han, S.; Liu, X.; Jin, X.; Zhang, F.; Zhou, M.; Guo, J. Variations of precipitable water vapor in sandstorm season determined from GNSS data: The case of China's Wuhai. *Earth Planets Space* **2023**, *75*, 126. [CrossRef]
4. Sapucci, L.F. Evaluation of modeling water-vapour-weighted mean tropospheric temperature for GNSS-integrated water vapour estimates in Brazil. *J. Appl. Meteorol. Climatol.* **2014**, *53*, 715–730. [CrossRef]
5. Zhu, D.; Sun, P.; Hu, Q.; Zhang, K.; Wu, S.; He, P.; Yu, A.; Yin, W.; Liu, W. A fusion framework for producing an accurate PWV map with spatiotemporal continuity based on GNSS, ERA5 and MODIS data. *IEEE Trans. Geosci. Remote Sens.* **2024**, *62*, 5802214. [CrossRef]
6. Zhu, D.; Zhang, K.; Sun, P.; Wu, S.; Wan, M. Homogenization of daily precipitable water vapor time series derived from GNSS observations over China. *Adv. Space Res.* **2023**, *72*, 1751–1763. [CrossRef]
7. Sun, Z.; Zhang, B.; Yao, Y. A Global Model for Estimating Tropospheric Delay and Weighted Mean Temperature Developed with Atmospheric Reanalysis Data from 1979 to 2017. *Remote Sens.* **2019**, *11*, 1893. [CrossRef]
8. Emardson, T.R.; Derks, H. On the relation between the wet delay and the integrated precipitable water vapour in the european atmosphere. *Meteorol. Appl.* **2010**, *7*, 61–68. [CrossRef]
9. He, C.; Wu, S.; Wang, X.; Hu, A.; Zhang, K. A new voxel-based model for the determination of atmospheric weighted mean temperature in GPS atmospheric sounding. *Atmos. Meas. Tech.* **2017**, *10*, 2045–2060. [CrossRef]
10. Baldysz, Z.; Nykiel, G. Improved Empirical Coefficients for Estimating Water Vapor Weighted Mean Temperature over Europe for GNSS Applications. *Remote Sens.* **2019**, *11*, 1995. [CrossRef]
11. Wang, X.; Zhang, K.; Wu, S.; Fan, S.; Cheng, Y. Water vapor-weighted mean temperature and its impact on the determination of precipitable water vapor and its linear trend. *J. Geophys. Res. Atmos.* **2016**, *121*, 833–852. [CrossRef]
12. Cai, M.; Li, J.; Liu, L.; Huang, L.; Zhou, L.; Huang, L.; He, H. Weighted Mean Temperature Hybrid Models in China Based on Artificial Neural Network Methods. *Remote Sens.* **2022**, *14*, 3762. [CrossRef]
13. Zhang, B.; Guo, Z.; Liu, X.; Shen, Y.; Yan, J.; Xu, F.; Cui, Y. Bevis Refined Model of Weighted Average Temperature in Hong Kong Considering Multi-Factors. *J. Xinyang Norm. Univ. (Nat. Sci. Ed.)* **2023**, *36*, 269–273.
14. Huang, L.; Jiang, W.; Liu, L.; Chen, H.; Ye, S. A new global grid model for the determination of atmospheric weighted mean temperature in GPS precipitable water vapor. *J Geod.* **2019**, *93*, 159–176. [CrossRef]
15. Li, Q.; Yuan, L.; Chen, P.; Jiang, Z. Global grid-based Tm model with vertical adjustment for GNSS precipitable water retrieval. *GPS Solut.* **2020**, *24*, 73. [CrossRef]
16. Bevis, M.; Businger, S.; Herring, A.T.; Rocken, C.; Anthes, R.A.; Ware, R.H. GPS meteorology: Remote sensing of atmospheric water vapor using the global positioning system. *J. Geophys. Res. Atmos.* **1992**, *97*, 15787–15801. [CrossRef]
17. Mekik, C.; Deniz, I. Modelling and validation of the weighted mean temperature for Turkey. *Meteorol. Appl.* **2017**, *24*, 92–100. [CrossRef]
18. Lan, Z.; Zhang, B.; Geng, Y. Establishment and analysis of global gridded Tm–Ts relationship model. *Geod. Geodyn.* **2016**, *7*, 101–107. [CrossRef]
19. Li, L.; Li, Y.; He, Q.; Wang, X. Weighted Mean Temperature Modelling Using Regional Radiosonde Observations for the Yangtze River Delta Region in China. *Remote Sens.* **2022**, *14*, 1909. [CrossRef]
20. Yao, Y.B.; Zhang, B.; Xu, C.Q.; Yan, F. Improved one/multi-parameter models that consider seasonal and geographic variations for estimating weighted mean temperature in ground-based GPS meteorology. *J Geod.* **2014**, *88*, 273–282. [CrossRef]
21. Yang, F.; Guo, J.; Meng, X.; Shi, J.; Zhang, D. Determination of Weighted Mean Temperature (Tm) Lapse Rate and Assessment of Its Impact on Tm Calculation. *IEEE Access* **2019**, *7*, 155028–155037. [CrossRef]
22. Huang, L.; Liu, L.; Chen, H.; Jiang, W. An improved atmospheric weighted mean temperature model and its impact on GNSS precipitable water vapor estimates for China. *GPS Solut.* **2019**, *23*, 51. [CrossRef]
23. Zhang, B.; Wang, Z.; Li, W.; Jiang, W.; Shen, Y.; Zhang, Y.; Zhang, S.; Tian, K. An Improved Spatiotemporal Weighted Mean Temperature Model over Europe Based on the Nonlinear Least Squares Estimation Method. *Remote Sens.* **2022**, *14*, 3609. [CrossRef]

24. Boehm, J.; Heinkelmann, R.; Schuh, H. Short note: A global model of pressure and temperature for geodetic applications. *J. Geod.* **2007**, *81*, 679–683. [CrossRef]
25. Lagler, K.; Schindelegger, M.; Böhm, J.; Krásná, H.; Nilsson, T. GPT2: Empirical slant delay model for radio space geodetic techniques. *Geophys. Res. Lett.* **2013**, *40*, 1069–1073. [CrossRef]
26. Böhm, J.; Möller, G.; Schindelegger, M.; Pain, G.; Weber, R. Development of an improved empirical model for slant delays in the troposphere (GPT2w). *GPS Solut.* **2015**, *19*, 433–441. [CrossRef]
27. Landskron, D.; Böhm, J. VMF3/GPT3: Refined discrete and empirical troposphere mapping functions. *J. Geod.* **2018**, *92*, 349–360. [CrossRef]
28. Yao, Y.; Zhu, S.; Yue, S. A globally applicable, season-specific model for estimating the weighted mean temperature of the atmosphere. *J. Geod.* **2012**, *86*, 1125–1135. [CrossRef]
29. Yao, Y.; Zhang, B.; Yue, S.; Xu, C.; Peng, W. Global empirical model for mapping zenith wet delays onto precipitable water. *J. Geod.* **2013**, *87*, 439–448. [CrossRef]
30. Yao, Y.; Xu, C.; Zhang, B.; Cao, N. GTm-III: A new global empirical model for mapping zenith wet delays onto precipitable water vapour. *Geophys. J. Int.* **2018**, *197*, 202–212. [CrossRef]
31. Mateus, P.; Mendes, V.B.; Plecha, S.M. HGPT2: An ERA5-Based Global Model to Estimate Relative Humidity. *Remote Sens.* **2021**, *13*, 2179. [CrossRef]
32. Levenberg, K. A method for the solution of certain problems in least squares. *Q. Appl. Math.* **1944**, *2*, 164–168. [CrossRef]
33. Marquardt, W. An algorithm for least-squares estimation of nonlinear parameters. *J. Soc. Ind. Appl. Math.* **1963**, *11*, 431–441. [CrossRef]
34. Yang, F.; Guo, J.; Chen, M.; Zhang, D. Establishment and analysis of a refinement method for the GNSS empirical weighted mean temperature model. *Acta Geod. Cartogr. Sin.* **2022**, *51*, 2339–2345.

Disclaimer/Publisher's Note: The statements, opinions and data contained in all publications are solely those of the individual author(s) and contributor(s) and not of MDPI and/or the editor(s). MDPI and/or the editor(s) disclaim responsibility for any injury to people or property resulting from any ideas, methods, instructions or products referred to in the content.